

A New Proposal for Live Load Distribution Factors of Bridges with Transverse Beams

Mohammad Bagher Abrishamkar, Reza Kholghi, Shervin Maleki*

*Dept. of Civil Engineering, Sharif University of Technology, Tehran, Iran
E-mail: Hili1374@gmail.com; r.kholghi@sharif.edu; smaleki@sharif.edu (Corresponding author)*

Received: 20 April 2022; Accepted: 13 July 2022; Available online: 10 August 2022

Abstract: Many bridge superstructures use transverse beams as load carrying components. In these systems, usually the transverse beams are connected to the main longitudinal girders or trusses on the two sides of the bridge. Such systems are commonly used in plate girder, box girder, cable-stayed and truss bridges. The live load distribution factor (LLDF) for bridge superstructures with transverse beams in AASHTO-LRFD bridge design specification has remained unchanged for decades and is prescribed as a function of the distance between the transverse beams. However, for slab-beam superstructures in which longitudinal beams at close spacing carry the loads to the substructure, the LLDFs have gone through many changes throughout the years and in their current forms depend on many parameters such as concrete slab thickness, beam span, longitudinal beam stiffness as well as the distance between the longitudinal beams. This study investigates the factors affecting the LLDF for transverse beams and intends to obtain new equations similar to AASHTO's longitudinal beam equations. For this purpose, 3D finite element models of different sample bridges were developed and critical parameters affecting the LLDF were identified and varied. Accordingly, the LLDFs for moment and shear forces of transverse beams were obtained through regression analyses. The proposed equations have less than 3.1% of average error for the cases considered.

Keywords: Bridge superstructure; Live load distribution factor; Transverse beam; Finite element analysis.

1. Introduction

Slab-girder steel bridges are widely used throughout the world for short and medium spans. Most of these bridges comprise of a concrete deck supported on longitudinal steel beams. For longer spans the designer might choose to use transverse floor beams with or without longitudinal stringers underneath the concrete deck to transfer the loads to the sides of the bridge. This superstructure arrangement is very common in box-girder, plate-girder, steel arch, cable stayed and suspension bridges (see Figure 1). A basic need in designing the longitudinal or transverse floor beams is the knowledge of the fraction of live load (design truck) that they receive from the concrete deck above. Most bridge design codes provide the live load distribution factors (LLDFs) to determine the share of the live load for the floor beams in different superstructure arrangements. The latest edition of AASHTO-LRFD Bridge Design Specifications [1] (from now on noted as AASHTO for short) contains detailed equations of LLDFs for the longitudinal beams of various types of bridge superstructures (Table 4.6.2.2.2 of AASHTO). For superstructures in which longitudinal beams at close spacing carry the loads to the substructure, the LLDFs have gone through many changes throughout the years and in its current forms depend on many parameters such as concrete slab thickness, beam span, longitudinal beam stiffness as well as the distance between the longitudinal beams. However, if the bridge deck is directly supported by transverse beams and the live load is transferred through these beams to the main side girders, the suggested equations for calculation of LLDFs for transverse beams are very simple and consider only the spacing between the transverse floor beams.

In the old AASHTO-Standard Specifications [2] for all kinds of beams, and in the current AASHTO specification [1] for transverse beams, the equations for calculation of LLDFs are only a function of beam spacing, in the form of S/D , in which S is the transverse beam spacing and D is a constant. According to current AASHTO Table 4.6.2.2.2f-1, the LLDF for transverse beams with a concrete deck on top, is equal to $S/1.8$ (for $S \leq 1.8$ m). This shows that despite many changes in the design specification throughout the years the LLDFs for transverse beams have not changed for decades.

Many researchers have investigated the effects of other parameters (other than S) on the distribution factor of longitudinal supporting girders. Cheung et al., [3] have shown that the intermediate diaphragms contribute to better distribution of live loads to girders. In studies carried out by Bishara et al. [4], 36 bridges with different span lengths, widths, and skew angles have been analyzed by the finite element (FE) method. Based on the results, it

has been concluded that the LLDF, especially for skewed bridges, has a lower value compared to the value given in AASHTO-Standard. Also, span lengths and bridge widths have a minor effect on the LLDF.



Figure 1. Typical bridge superstructures with transverse floor beams; (a) Steel arch bridge, (b) Steel box girder bridge

Zokaie [5] suggested equations for calculation of LLDFs through analyzing constructed bridges across the USA by the finite element method for standard design truck of AASHTO considering the mentioned parameters. These equations were incorporated in AASHTO specifications. Cai [6] has investigated the effect of diaphragms on the distribution of live loads between girders in slab-girder bridges and suggested a modification factor to improve the accuracy of AASHTO equations by considering the effect of the internal diaphragms on LLDF. Patrick et al. [7] investigated the lateral spacing of the design trucks in loaded lanes on LLDF by FE analyses of steel and concrete bridges. The results have shown that the lateral spacing of design trucks doesn't have a considerable effect on LLDF. Barr & Amin [8] have studied the effect of beam spacing, span length, overhang length and skew angle on the LLDFs for shear in girders by FE simulation of more than 200 single span bridges and concluded that increasing beam spacing is the most significant factor that affects the shear LLDF for interior girders and for exterior girders shear LLDF is mainly affected by overhang length. Longitudinal stiffness of beams is one of the influential parameters in calculation of the LLDF that its value is unknown before design. Phuvoravan [9] suggested an equation for LLDF based on the results of FE simulation of 43 bridges that is independent of stiffness parameter to avoid trial and error process in design.

Besides the geometric and stiffness properties of the superstructure, the type and geometry of the applied live load is also important in the distribution of live load among girders. So, many researchers have investigated the distribution of live load for different types of design live load. Tabsh & Tabatabai [10] studied the effect of oversized design trucks with 3 different widths on LLDF through FE analyses of the bridges used in research by Zokaie [5]. Bae & Michael [11] and Kilaru [12] investigated the distribution factor for truck overloads and farm vehicles. The results showed that the standard design truck of AASHTO has the most critical values of LLDF. Distribution factors have also been studied for pre-tensioned concrete box-girder bridges. The results of studies carried out by Hughs & Idriss [13] showed that LLDFs calculated by the equations given in AASHTO are conservative compared to the results of FE analyses. More recently, research on LLDF has considered specific bridge systems with longitudinal beams [14-20].

As noted above, many researchers have investigated the effect of different parameters on LLDFs for longitudinal girders. The finite element modeling has been used in majority of these researches. However, the evaluation of effective parameters influencing the LLDFs for transverse supporting beams is scarce in the literature. Pennings et al. [20] suggested an equation for calculation of distribution factor of the transverse beams that are not connected directly to the deck. In their study, details of 12 constructed bridges in Texas, USA, were used, in which, the applied live load to bridge deck was first transferred to longitudinal stringers, and then through transverse beams it reaches the main longitudinal girders. Yet, further investigation of distribution factors for common bridge systems in which the deck is directly supported by transverse beams was not considered.

The main purpose of this research is to develop LLDF equations for transverse beams considering all the critical parameters in the exact same manner that the LLDF equations of AASHTO for longitudinal beams were developed (AASHTO Table 4.6.2.2.2). For this purpose, 3D finite element (FE) models of typical bridges with transverse floor beams were constructed. The design truck of AASHTO was placed in the most critical location on the deck and the moment and shear forces in the transverse beams were obtained. Equations for LLDF were derived from analyses of many bridges with variable parameters using regression. It is shown that the derived equations can estimate the internal forces in the transverse beams accurately in all usual cases encountered in practice.

2. Finite element modeling

2.1 Bridge models

Simulation and analysis of bridge models were carried out using CSiBridge finite element software [21]. In order to reduce the computational cost and considering that the substructure has no effect on the results, only the superstructure of the bridges was modeled. As shown in Figure 2, the superstructure for all models is a single span, simply supported slab-girder system that consists of two main longitudinal girders on the sides of the superstructure. The closely spaced transverse floor beams are simply supported by the main girders. The transverse beam and longitudinal girder sizes and FE models are shown in Fig.2. The non-composite model uses a rigid link between the centroids of the deck and the beam with the vertical degree of freedom restrained. In composite models the longitudinal degree of freedom of the link is also restrained. The steel grade is 50 ksi with yield strength of 350 MPa. The concrete deck 28 days compressive strength is 28 MPa.

All models have two standard design lanes, each 3.6 m wide according to the AASHTO specifications. Hence, the total widths of superstructures range from 7.2 m to 10.8 m depending on the overhang widths on each side. The influence of all parameters that are most likely to affect the distribution factors have been investigated through analyzing bridge models with varying values assigned to each parameter. The assumed critical variable parameters throughout the finite element analyses include concrete slab thickness (t_s), spacing of transverse beams (S), length of transverse beams (l), stiffness of transverse beams (k_g), bridge span (L), longitudinal stiffness of longitudinal girders (K_G), the effect of composite action between the concrete deck and steel beams. Fig. 3 depicts the parameters involved.

In order to obtain a better understanding of correlation between LLDFs and each variable parameter, FE analyses models were categorized into 6 sets, such that in each set only one variable parameter was changed, and the others were kept constant. Details of the bridge models are presented in Table 1. Although there are 22 models listed in this table, some of the models in each set have similar properties. Also, note that some variable parameters are interdependent. For example, an increase in slab thickness might change the transverse beam and longitudinal girder size and stiffness.

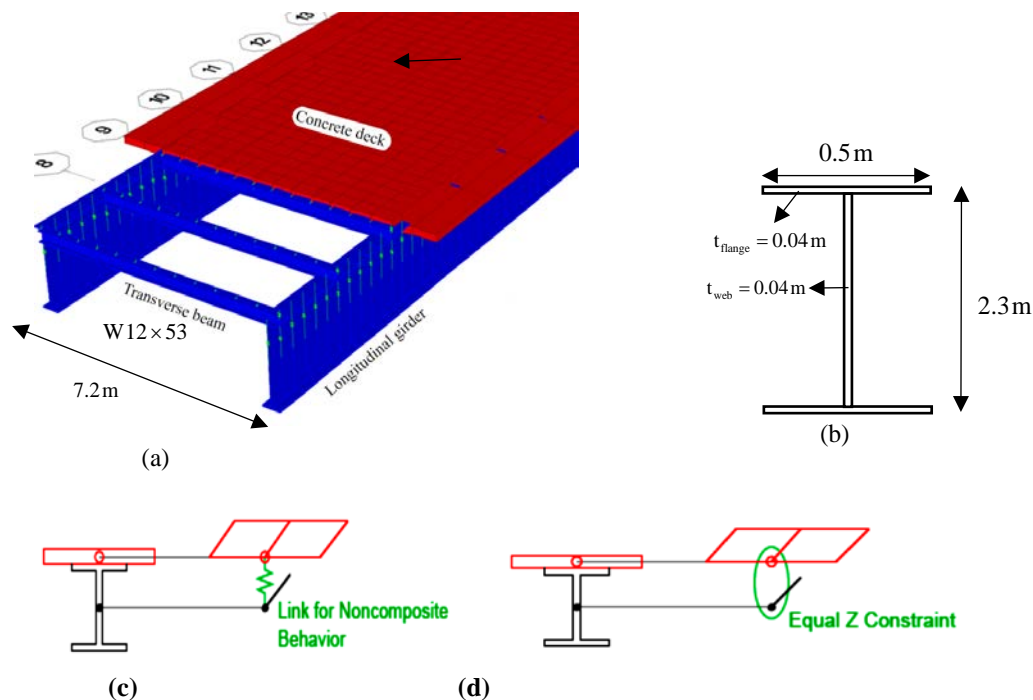


Figure 2. Superstructure FE model a) 3D view, b) Longitudinal girder section, c) Slab-beam model for NC type, d) Slab-beam model for C type

2.2 Load application

The live load applied in the analysis and design of bridges was in accordance with AASHTO specification. Accordingly, vehicular live load consists of two types of vehicles: a design truck (HL-93K), or a design tandem (HL-93M), both of which are combined with a distributed lane load. The vehicular live loads should be positioned such that the most critical shear and moment is produced in the bridge component.

As shown in Fig. 4, the design truck consists of two 145 kN axle loads with variable spacing between 4.2 m to 9 m and one 36 kN axle load with 4.2 m spacing in front of the truck. Design tandem consists of two 110 kN axle loads with 1.2 m spacing. The additional lane load for both loadings is a 9.3 kN/m uniformly distributed load in the longitudinal direction. All loads occupy a width of 3.0 m in the transverse direction. The wheel loads should not get closer than 0.6 m to the curbs.

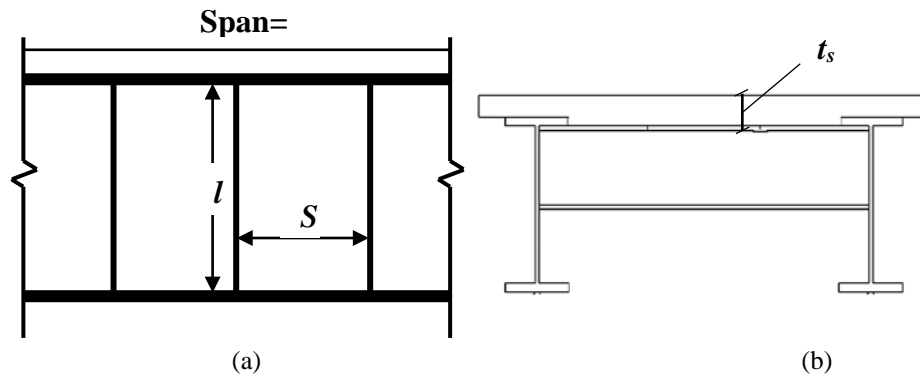


Figure 3. Graphical presentation of variable parameters; (a) Plan view, (b) Elevation view

Table 1. Details of bridge models for FE analyses

Set No.	Model ID	Spacing of transverse beams, S (m)	Slab thickness, t_s (mm)	Length of longitudinal girders, L (m)	Length of transverse beams, l (m)	stiffness of transverse beams, K_g (mm^4)	stiffness of longitudinal girders, K_G (mm^4)
1	1-1	2.25	200	54	7.2	6.6×10^9	1.47×10^{12}
	1-2	1.8	200	54	7.2	6.6×10^9	1.47×10^{12}
	1-3	2.7	200	54	7.2	6.6×10^9	1.47×10^{12}
	1-4	1.5	200	54	7.2	6.6×10^9	1.47×10^{12}
2	2-1	2.25	200	54	7.2	6.6×10^9	1.47×10^{12}
	2-2	2.25	220	54	7.2	7.01×10^9	1.48×10^{12}
	2-3	2.25	250	54	7.2	7.67×10^9	1.51×10^{12}
	2-4	2.25	180	54	7.2	6.2×10^9	1.45×10^{12}
3	3-1	2.25	250	54	7.2	7.67×10^9	1.51×10^{12}
	3-2	2.25	250	54	7.2	9.08×10^9	1.51×10^{12}
	3-3	2.25	250	54	7.2	1.19×10^{10}	1.51×10^{12}
4	4-1	2.25	250	54	7.2	7.67×10^9	1.8×10^{12}
	4-2	2.25	250	54	8.4	7.67×10^9	1.8×10^{12}
	4-3	2.25	250	54	9.6	7.67×10^9	1.8×10^{12}
	4-4	2.25	250	54	7.8	7.67×10^9	1.8×10^{12}
	4-5	2.25	250	54	9	7.67×10^9	1.8×10^{12}
5	5-1	2.25	250	54	7.2	7.67×10^9	1.8×10^{12}
	5-2	2.25	250	54	7.2	7.67×10^9	1.99×10^{12}
	5-3	2.25	250	54	7.2	7.67×10^9	2.18×10^{12}
6	6-1	2.25	200	54	7.2	6.6×10^9	1.47×10^{12}
	6-2	2.25	200	45	7.2	6.6×10^9	1.47×10^{12}
	6-3	2.25	200	36	7.2	6.6×10^9	1.47×10^{12}

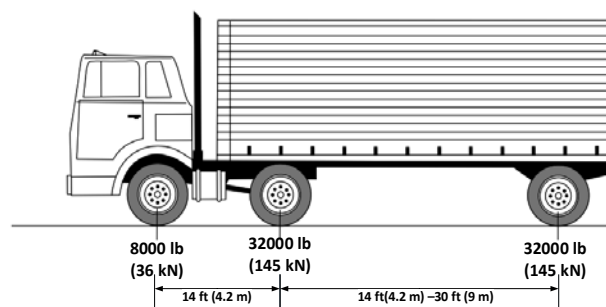


Figure 4. Characteristics of design truck live load [1]

In this research, the determination of the LLDFs was only based on the HL-93K loading which controls all cases considered. However, all FE models were initially designed in compliance with AASHTO for both types of vehicular live loads with corresponding LLDFs.

Since all models have two design lanes, four wheel loads are considered for the calculation of LLDFs. The position of wheel loads corresponding to maximum live moment and shear in transverse beams is determined based on the structural analysis as shown in Figure 5, where W indicates 145 kN axle load. Critical position of wheel loads resulting in maximum moment in transverse beams occurs when the resultant of wheel loads ($R=2W$) and a near wheel load are at equal distance from the centerline of the transverse beam. In case of shear, the critical position of wheel loads is when the loads are shifted to one end of the transverse beam. However, the wheels cannot get closer than 0.6 m from the edge of the sidewalks.

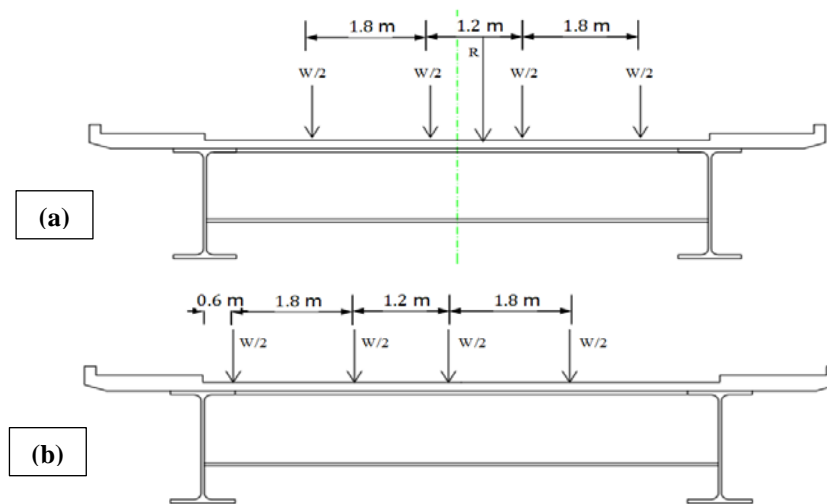


Figure 5: Critical position of the wheel loads on the transverse beam for a) maximum moment and b) maximum shear

3. Analysis results and discussion

The results of the FE analyses to calculate LLDFs for moment and shear in transverse floor beams are presented in this section. The equations for LLDFs in each case were obtained through nonlinear regression analysis considering the critical parameters noted in section 2.1. Furthermore, the effect of composite action between the concrete deck and steel beams was also investigated by analyzing the FE models with both composite and non-composite sections.

3.1 LLDF for moment

There are several methods available for the calculation of LLDFs based on the results of a 3D FE model. In this research, LLDFs for bending moment were determined by calculating the ratio of maximum live load moment in the most critical transverse beam to total live load moments in all transverse beams.

The distribution factors were investigated for transverse beams in the middle region of the bridge span and also for transverse beams near the ends of the bridge span. Comparison of the LLDFs for these two cases showed that the difference is negligible. Furthermore, LLDFs were also investigated for transverse beams located on top of the abutments where a cross-frame diaphragm existed between the beams. It was concluded that due to diaphragm stiffness LLDFs for such beams were considerably different from other transverse beams.

Figure 6 shows the analyses results for moment LLDF of transverse beams with composite section. For each chart a trend line using power function has been fitted to the obtained data points. Power function can be represented in the form of Eq. (1) that is a single term function with constant power (b) and multiplier (a).

$$y = ax^b \quad (1)$$

The obtained results shown in Fig.6 indicate that the spacing (S) and the length of transverse beams (l) have a major effect on moment distribution factor. However, the effects of longitudinal stiffness of girders and bridge span are negligible and can be ignored.

The results of nonlinear regression analysis for parameter (b) in power function is presented in Table 2. As a result, the relation between moment distribution factor for transverse beams with composite sections (MC) and a

combination of influential parameters can be expressed as:

$$(LLDF)_{MC} \propto (S)^{0.49}(t_s)^{-0.38}(K_g)^{0.06}(l)^{-0.58} \tag{2}$$

Table 2. Calculated values for constant power parameter (b) in power functions using nonlinear regression

Parameter	MC	MNC	VC	VNC
S	0.49	0.8	0.51	0.58
t_s	-0.38	-0.26	-0.38	0.03
l	-0.58	-0.9	-0.25	-0.24
K_g	0.06	0.35	0.02	0.09

*MC=moment in composite beam; MNC=moment in noncomposite beam; VC= shear in composite beam; VNC=shear in noncomposite beam

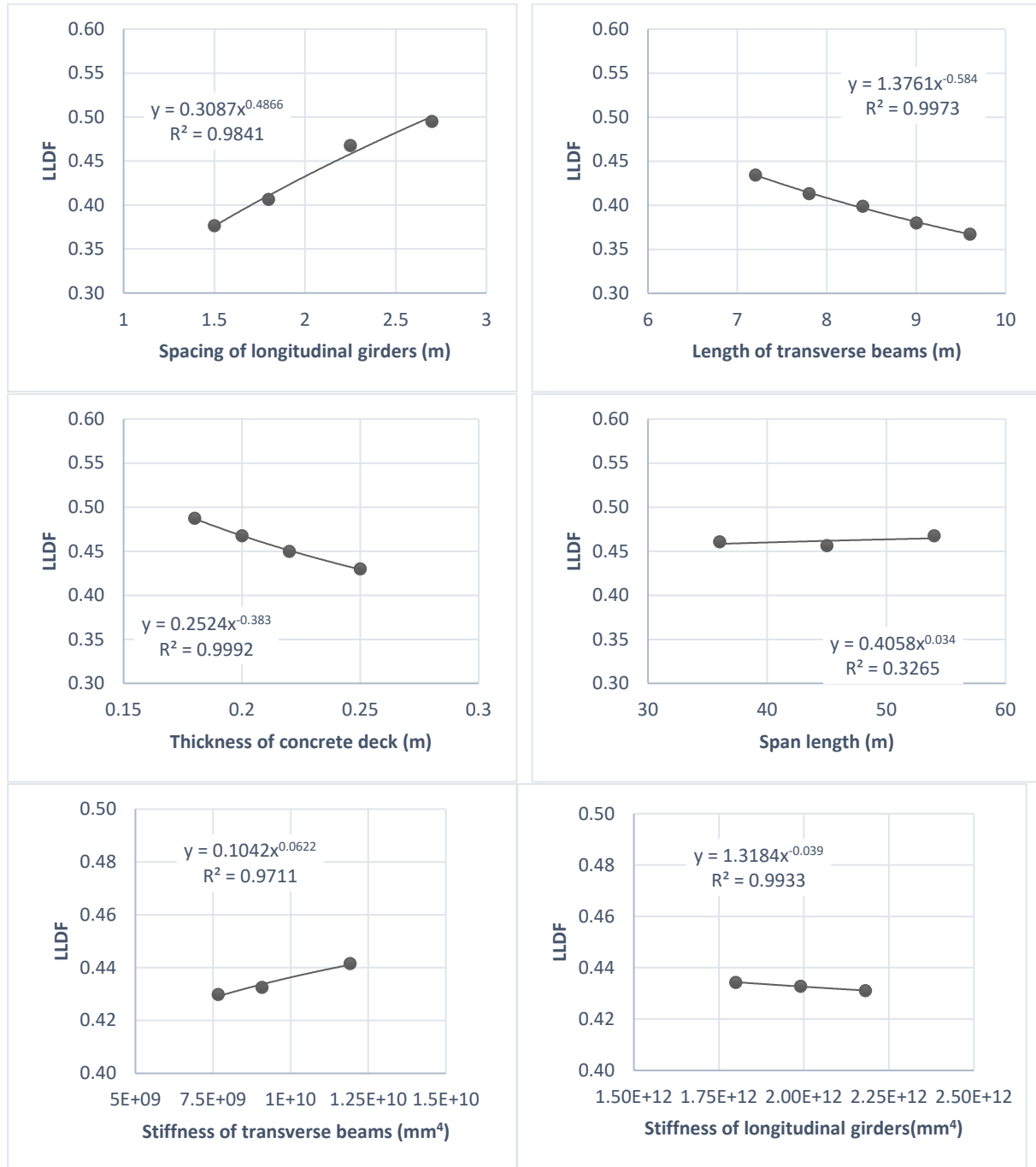


Figure 6. Live load distribution factors for moment in transverse beams with composite section

In the case of non-composite sections, the maximum value of moment in transverse beams is higher than the composite sections. Thus, according to Table 2, the relation between bending moment LLDF for transverse beams with non-composite sections using a combination of influential parameters can be expressed as:

$$(LLDF)_{MNC} \propto (S)^{0.8}(t_s)^{-0.26}(K_g)^{0.35}(l)^{-0.9} \quad (3)$$

Furthermore, Eq. (4) is derived from Eq. (2) in a similar form as in AASHTO by keeping the power of S (the most critical parameter) and by slight manipulation of powers of other parameters. Similarly, Eq. (5) is derived from Eq. (3) for non-composite sections.

$$(LLDF)_{MC} = a_1 + \left(\frac{a_2}{l}\right)^{0.1} \left(\frac{S}{l}\right)^{0.49} \left(\frac{K_g}{(t_s)^4}\right)^{0.09} \quad (4)$$

$$(LLDF)_{MNC} = a_1 + \left(\frac{S}{a_2}\right)^{0.8} \left(\frac{K_g}{l^3 t_s \times 10^9}\right)^{0.3} \quad (5)$$

In these equations, S and l are spacing and length of transverse beams in meters, K_g is longitudinal stiffness of transverse beams in mm^4 and t_s is concrete slab thickness in mm. The a_1 and a_2 are constant parameters that should be determined by trial and error for each equation to best match the results of FE analyses. Accordingly, the final form of the proposed LLDF equations for moment can be expressed as:

$$(LLDF)_{MC} = 0.05 + \left(\frac{0.1}{l}\right)^{0.1} \left(\frac{S}{l}\right)^{0.49} \left(\frac{K_g}{(t_s)^4}\right)^{0.09} \quad (6)$$

$$(LLDF)_{MNC} = 0.05 + \left(\frac{S}{0.35}\right)^{0.8} \left(\frac{K_g}{l^3 t_s \times 10^9}\right)^{0.3} \quad (7)$$

3.2 LLDF for shear

The obtained results from FE analyses were used to calculate shear LLDF for the considered bridges of Table 1. A similar procedure to moment distribution factor was used except that the critical position of wheel loads on the transverse beams were different (see Fig.5b).

The obtained shear LLDF for the composite bridges considered are plotted in Fig. 7 against each variable parameter. These charts illustrate that the shear LLDF mainly depends on the length and spacing of transverse beams. Meanwhile, it can be concluded that variation of bridge span, longitudinal stiffness of girders and floor beams for both types of composite and non-composite sections and, also concrete slab thickness (in case of non-composite beams), don't have a considerable effect on the shear LLDF. The results of nonlinear regression analysis for parameter (b) in the power function is presented in Table 2. Thus, the relation between shear LLDF and influential parameters can be expressed as:

1) for transverse beams with composite section,

$$(LLDF)_{VC} \propto (S)^{0.51}(t_s)^{-0.38}(l)^{-0.25} \quad (8)$$

2) For transverse beams with non-composite section,

$$(LLDF)_{VNC} \propto (S)^{0.58}(l)^{-0.24} \quad (9)$$

Based on the obtained results, equations are proposed for calculation of shear LLDF in transverse beams in a similar form as in AASHTO. As a result of applying this procedure, the proposed equations for calculation of shear distribution factor for transverse beams with composite and non-composite section are presented in Eq. (10) and Eq. (11), respectively.

$$(LLDF)_{VC} = a_1 + \left(\frac{S}{a_2}\right)^{0.25} \left(\frac{S}{l}\right)^{0.27} \left(\frac{a_3}{t_s}\right)^{0.28} \quad (10)$$

$$(LLDF)_{VNC} = a_1 + \left(\frac{S}{a_2}\right)^{0.32} \left(\frac{S}{l}\right)^{0.26} \quad (11)$$

In these expressions, a_1 , a_2 and a_3 are constant parameters that should be determined by trial and error and other parameters are as defined before. Finally, the proposed equations are expressed as:

$$(LLDF)_{VC} = 0.05 + \left(\frac{S}{0.2}\right)^{0.25} \left(\frac{S}{l}\right)^{0.27} \left(\frac{2}{0.1 t_s}\right)^{0.28} \quad (12)$$

$$(LLDF)_{VNC} = 0.05 + \left(\frac{S}{35}\right)^{0.32} \left(\frac{S}{l}\right)^{0.26} \tag{13}$$

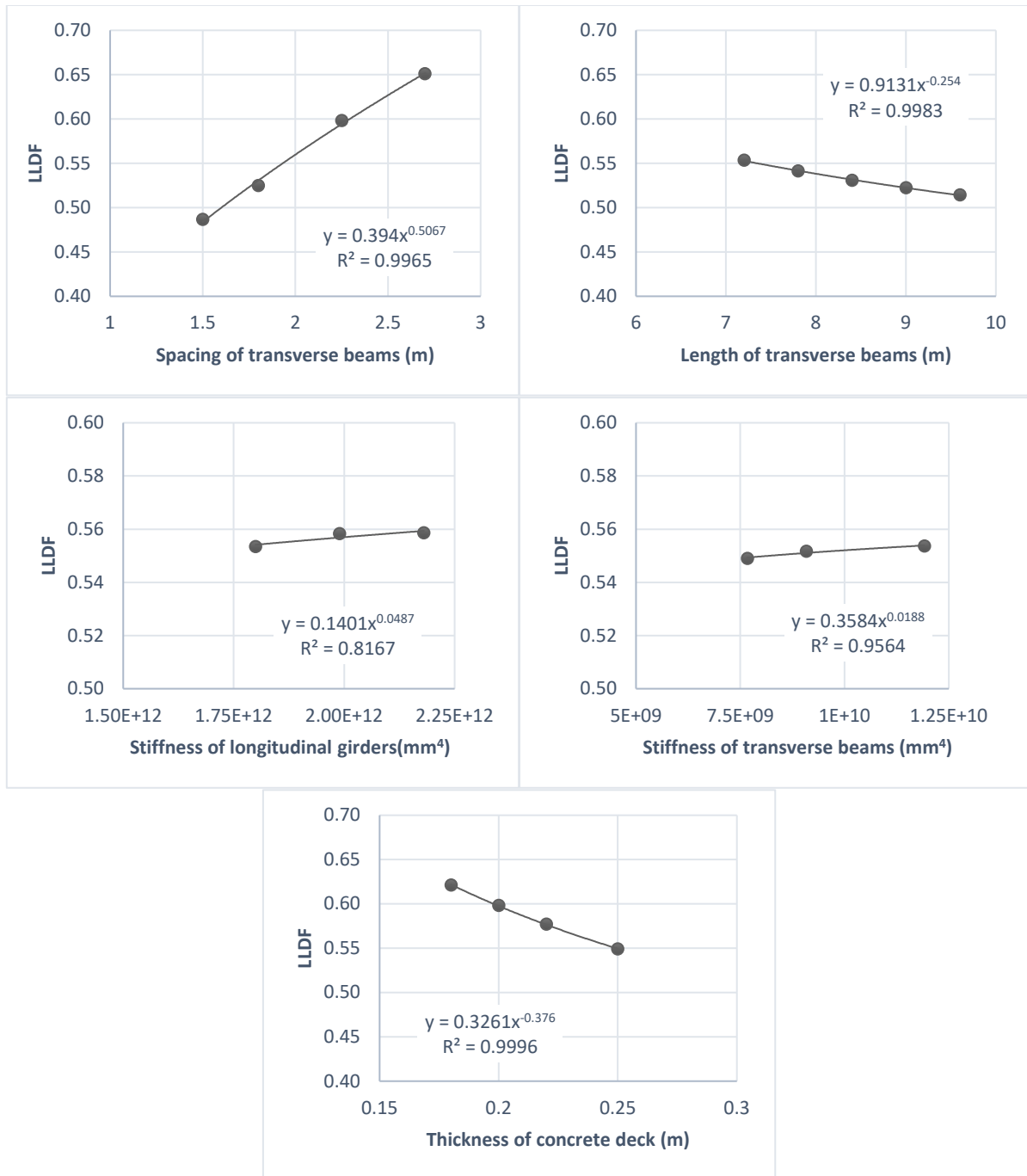


Figure 7. Live load distribution factors for shear in transverse beams with composite section

3.3 Validation of the proposed equations

The most accurate method for determination of LLDFs that can be used for any configuration of superstructure is through FE modeling and analysis of the bridge system under live loads. Obviously, the 3D FE model is more accurate than other models. However, it is more practical to use prescribed equations such as the equations proposed in this research that have been developed based on the results of FE analyses for a vast number of models considering all the critical parameters. As such, the more FE models (representing actual bridges in practice) are built and investigated, the more dependable the results and the proposed equations will be. The results of FE analyses and values obtained from the proposed equations for moment and shear LLDFs with composite and non-composite sections are shown and compared in Table 3. It can be seen that the LLDFs calculated by the proposed equations have higher values compared to the results of FE analyses, thus, it can be concluded that the proposed

equations are conservative to use in all cases. The maximum average error is only 3.1% and belongs to LLDF for moment in non-composite transverse beams.

Considering the properties of the models, we note that the spacing of transverse beams for most of the models is outside the range of applicability of AASHTO equations and lever rule applies. Also, for the lever rule method, the critical position for the axle load of the design truck is when the axle load is located directly on the transverse beam so, the LLDF is 1.0 for all models according to AASHTO. Table 4 compares these values with the proposed equations of this paper. It can be seen that the current AASHTO equations are overly conservative and lead to uneconomical designs.

Table 3. Comparison between the LLDF results based on the FE analyses and the proposed equations

Model ID	Moment LLDF						Shear LLDF					
	Composite			Non-composite			Composite			Non-composite		
	Eq. (6)	FEM	Error (%)	Eq. (7)	FEM	Error (%)	Eq. (12)	FEM	Error (%)	Eq. (13)	FEM	Error (%)
1 – 1	0.47	0.47	0	0.32	0.32	0	0.61	0.60	2	0.36	0.36	0
1 – 2	0.43	0.41	5	0.28	0.26	6	0.55	0.52	4	0.32	0.30	6
1 – 3	0.51	0.50	3	0.36	0.36	1	0.66	0.65	2	0.39	0.39	0
1 – 4	0.39	0.38	4	0.24	0.23	8	0.50	0.49	3	0.29	0.28	4
2 – 1	0.47	0.47	0	0.32	0.32	0	0.61	0.60	2	0.36	0.36	0
2 – 2	0.46	0.45	2	0.32	0.31	2	0.59	0.58	2	0.36	0.36	0
2 – 3	0.44	0.43	3	0.31	0.30	3	0.56	0.55	2	0.36	0.36	2
2 – 4	0.48	0.49	1	0.32	0.33	2	0.63	0.62	2	0.36	0.36	1
3 – 1	0.43	0.43	1	0.31	0.30	3	0.56	0.55	2	0.36	0.36	2
3 – 2	0.45	0.43	4	0.33	0.32	1	0.56	0.55	2	0.36	0.36	2
3 – 3	0.46	0.44	4	0.35	0.35	1	0.56	0.55	2	0.36	0.38	6
4 – 1	0.44	0.43	2	0.31	0.30	4	0.56	0.55	2	0.36	0.36	1
4 – 2	0.41	0.40	2	0.28	0.27	2	0.54	0.53	2	0.35	0.34	1
4 – 3	0.38	0.37	4	0.25	0.24	8	0.52	0.51	2	0.33	0.34	0
4 – 4	0.42	0.41	3	0.30	0.29	3	0.55	0.54	2	0.35	0.35	0
4 – 5	0.39	0.38	4	0.27	0.25	8	0.53	0.52	2	0.34	0.34	0
5 – 1	0.44	0.43	2	0.31	0.30	4	0.56	0.55	2	0.36	0.36	1
5 – 2	0.44	0.43	2	0.31	0.30	4	0.56	0.56	1	0.36	0.35	1
5 – 3	0.44	0.43	3	0.31	0.30	5	0.56	0.56	1	0.36	0.35	1
6 – 1	0.47	0.47	0	0.32	0.32	0	0.61	0.6	2	0.36	0.36	0
6 – 2	0.47	0.46	3	0.32	0.32	0	0.61	0.6	1	0.36	0.36	0
6 – 3	0.47	0.46	2	0.32	0.32	1	0.61	0.6	1	0.36	0.36	0
average	-	-	2.3	-	-	3.1	-	-	1.8	-	-	1.3

4. Conclusions

This study developed new live load distribution factors (LLDFs) for slab-girder bridges with transverse beams at equal spacing. The transverse beams could be composite or non-composite. Finite element simulations were carried out to study the influence of several parameters on the variation of moment and shear LLDFs. The critical variable parameters were transverse beam spacing, concrete slab thickness, bridge span, transverse beam length, stiffness of longitudinal girders and transverse beams. The main outcomes of this study can be summarized as follows:

1) The results indicate that the transverse beam length is the most influential parameter on the variation of bending moment distribution factor. Also, it has been shown that length and longitudinal stiffness of girders have minor effect on the variation of bending moment distribution factor and can be neglected in the proposed equations. Based on the results of the finite element analyses, two LLDF equations have been proposed for moment in transverse beams with composite and non-composite actions, as indicated by Eqs. (6) and (7), respectively. The maximum average error of the proposed equations is 3.1% with respect to FE results.

2) The distribution factor for shear force in the transverse beam were obtained for both composite and non-composite transverse beams. Based on the obtained results, transverse beam spacing was the main parameter affecting the shear LLDF. Also, it was shown that, in addition to length and longitudinal stiffness of girders, the effect of concrete slab thickness and longitudinal stiffness of transverse beams could be neglected. Proposed LLDF equations for shear in transverse beams with composite and non-composite actions, were presented by Eqs. (12) and (13), respectively. The maximum average error of the proposed equations is 1.8% with respect to FE results.

3) The proposed equations are much better than the current AASHTO procedure and lead to more economical designs. On average, up to 56% reduction in moment and 43% reduction in shear load calculations can be obtained by using the proposed equations of this paper and still be on the conservative side.

Table 4. Comparison between the LLDF obtained from the proposed equations and AASHTO specification

Model ID	Moment LLDF						Shear LLDF					
	Composite			Non-composite			Composite			Non-composite		
	Eq. (6)	AASHTO	Error (%)	Eq. (7)	AASHTO	Error (%)	Eq. (12)	AASHTO	Error (%)	Eq. (13)	AASHTO	Error (%)
1-1	0.47	1	53%	0.32	1	68%	0.61	1	39%	0.36	1	64%
1-2	0.43	1	57%	0.28	1	72%	0.55	1	45%	0.32	1	68%
1-3	0.51	1	49%	0.36	1	64%	0.66	1	34%	0.39	1	61%
1-4	0.39	1	61%	0.24	1	76%	0.5	1	50%	0.29	1	71%
2-1	0.47	1	53%	0.32	1	68%	0.61	1	39%	0.36	1	64%
2-2	0.46	1	54%	0.32	1	68%	0.59	1	41%	0.36	1	64%
2-3	0.44	1	56%	0.31	1	69%	0.56	1	44%	0.36	1	64%
2-4	0.48	1	52%	0.32	1	68%	0.63	1	37%	0.36	1	64%
3-1	0.43	1	57%	0.31	1	69%	0.56	1	44%	0.36	1	64%
3-2	0.45	1	55%	0.33	1	67%	0.56	1	44%	0.36	1	64%
3-3	0.46	1	54%	0.35	1	65%	0.56	1	44%	0.36	1	64%
4-1	0.44	1	56%	0.31	1	69%	0.56	1	44%	0.36	1	64%
4-2	0.41	1	59%	0.28	1	72%	0.54	1	46%	0.35	1	65%
4-3	0.38	1	62%	0.25	1	75%	0.52	1	48%	0.33	1	67%
4-4	0.42	1	58%	0.3	1	70%	0.55	1	45%	0.35	1	65%
4-5	0.39	1	61%	0.27	1	73%	0.53	1	47%	0.34	1	66%
5-1	0.44	1	56%	0.31	1	69%	0.56	1	44%	0.36	1	64%
5-2	0.44	1	56%	0.31	1	69%	0.56	1	44%	0.36	1	64%
5-3	0.44	1	56%	0.31	1	69%	0.56	1	44%	0.36	1	64%
6-1	0.47	1	53%	0.32	1	68%	0.61	1	39%	0.36	1	64%
6-2	0.47	1	53%	0.32	1	68%	0.61	1	39%	0.36	1	64%
6-3	0.47	1	53%	0.32	1	68%	0.61	1	39%	0.36	1	64%
average	-	-	56%	-	-	69%	-	-	43%	-	-	65%

5. Notation list

t_s	Concrete slab thickness
S	Spacing of transverse beams
l	Length of transverse beams
K_g	Stiffness of transverse beams
L	Length of longitudinal girders (bridge span)
K_G	Longitudinal stiffness of longitudinal girders
W	Truck wheel load (kN)
C	Composite section
NC	Non-composite section

6. References

- [1] AASHTO LRFD Bridge Design Specifications (9th ed.). The American Association of State Highway and Transportation Officials, 2020.
- [2] AASHTO Standard Specifications for Highway Bridges (17th ed.). The American Association of State Highway and Transportation Officials, 2002.
- [3] Cheung MS, Jategaonkar R, Jaeger LG. Effects of intermediate diaphragms in distributing live loads in beam-and-slab bridges. Canadian Journal of Civil Engineering. 1986; 13(3): 278–292. <https://doi.org/10.1139/l86-040>
- [4] Bishara AG, Chuan LM, El-Ali N. Wheel load distribution on simply supported skew I-beam composite bridges. Journal of Structural Engineering. 1993;119(2):399–419. [https://doi.org/10.1061/\(ASCE\)0733-9445\(1993\)119:2\(399\)](https://doi.org/10.1061/(ASCE)0733-9445(1993)119:2(399))
- [5] Zokaie T. AASHTO-LRFD live load distribution specifications. Journal of Bridge Engineering. 2000; 5(2): 131–138. [https://doi.org/10.1061/\(ASCE\)1084-0702\(2000\)5:2\(131\)](https://doi.org/10.1061/(ASCE)1084-0702(2000)5:2(131))

- [6] Cai CS. Discussion on AASHTO LRFD load distribution factors for slab-on-girder bridges. *Practice Periodical on Structural Design and Construction*, 2005; 10(3): 171–176. [https://doi.org/10.1061/\(ASCE\)1084-0680\(2005\)10:3\(171\)](https://doi.org/10.1061/(ASCE)1084-0680(2005)10:3(171))
- [7] Patrick MD, Huo XS, Jay P, Mertz, DM. Sensitivity of live load distribution factors to vehicle spacing. *Journal of Bridge Engineering*. 2006; 11(1): 131–134. [https://doi.org/10.1061/\(ASCE\)1084-0702\(2006\)11:1\(131\)](https://doi.org/10.1061/(ASCE)1084-0702(2006)11:1(131))
- [8] Barr PJ, Amin MD. Shear live-load distribution factors for I-girder bridges. *Journal of Bridge Engineering*. 2006; 11(2): 197–204. [https://doi.org/10.1061/\(ASCE\)1084-0702\(2006\)11:2\(197\)](https://doi.org/10.1061/(ASCE)1084-0702(2006)11:2(197))
- [9] Phuvoravan K. Load distribution factor equation for steel girder bridges in LRFD design. *Proc., Infrastructure Development and the Environment*. SEAMEO-INNOTECH, Quezon City, Philippines, 2006.
- [10] Tabsh SW, Tabatabai M. Live load distribution in girder bridges subject to oversized trucks. *Journal of Bridge Engineering*. 2001; 6(1): 9–16. [https://doi.org/10.1061/\(ASCE\)1084-0702\(2001\)6:1\(9\)](https://doi.org/10.1061/(ASCE)1084-0702(2001)6:1(9))
- [11] Bae HU, Michael OG. Moment and shear load distribution factors for multigirder bridges subjected to overloads. *Journal of Bridge Engineering*. 2012; 17(3): 519–527. [https://doi.org/10.1061/\(ASCE\)BE.1943-5592.0000271](https://doi.org/10.1061/(ASCE)BE.1943-5592.0000271)
- [12] Kilaru CT. Live load distribution factors for multi-span girder bridges with plank decking subjected to farm vehicles. [MS Thesis]. Iowa State University, 2015.
- [13] Hughs E, Idriss R. Live-load distribution factors for prestressed concrete spread box-girder bridge. *Journal of Bridge Engineering*. 2006; 11(5): 573–581. [https://doi.org/10.1061/\(ASCE\)1084-0702\(2006\)11:5\(573\)](https://doi.org/10.1061/(ASCE)1084-0702(2006)11:5(573))
- [14] Razzaq MK, Sennah K, Ghrib F. Live load distribution factors for simply-supported composite steel I-girder bridges. *Journal of Constructional Steel Research*. 2021;181:106612.
- [15] Sofi S, Steelman JS. Nonlinear flexural distribution behavior and ultimate system capacity of skewed steel girder bridges. *Engineering Structures*. 2019; 197. <https://doi.org/10.1016/j.engstruct.2019.109392>
- [16] Torres V, Zolghadri N, Maguire M, Barr P. Experimental and analytical investigation of live-load distribution factors for double Tee bridges. *ASCE- Journal of Performance of Constructed Facilities*. 2019; 33(1).
- [17] Choi W, Mohseni I, Park J, Kang J. Development of live load distribution factor equation for concrete multicell box-girder bridges under vehicle loading. *International Journal of Concrete Structures and Materials*. 2019; 13, Article number: 22.
- [18] Mohseni I, Cho YK, Kang J. Live load distribution factors for skew stringer bridges with high-performance steel girders under truck loads. *Applied Sciences*. 2018; 8(10):1717. DOI <https://doi.org/10.3390/app8101717>
- [19] Thakuria P, Talukdar S. Live load distribution factor in precast I-girder bridge. 14th International Conference on Concrete Engineering and Technology. IOP Conf. Series: Materials Science and Engineering. 2018; 431:11212.
- [20] Pennings KR, Frank KH, Wood SL, Yura JA, Jirsa JO. Lateral load distribution on transverse floor beams in steel plate girder bridges. Research Report 1746-3. Center for Transportation Research Bureau of Engineering Research. The University of Texas at Austin, 2000.
- [21] CSiBridge. Computer Software. Computers & Structures Inc. Walnut Creek, CA, 2019.



© 2022 by the author(s). This work is licensed under a [Creative Commons Attribution 4.0 International License](http://creativecommons.org/licenses/by/4.0/) (<http://creativecommons.org/licenses/by/4.0/>). Authors retain copyright of their work, with first publication rights granted to Tech Reviews Ltd.